Thin Solid Films 619 (2016) 214–219

Contents lists available at ScienceDirect

Thin Solid Films

journal homepage: www.elsevier.com/locate/tsf

Thickness dependence of electrical and piezoelectric properties of ferroelectric $Ba_{0.8}Sr_{0.2}TiO_3$ thin films

D.A. Kiselev [a,b,*], M.S. Afanasiev [b], S.A. Levashov [b], A.A. Sivov [b], G.V. Chucheva [b]

[a] National University of Science and Technology "MISiS", Leninskiy pr. 4, Moscow 119049, Russia
[b] Kotelnikov Institute of Radio Engineering and Electronics Russian Academy of Sciences (Fryazino Branch), pl. Vvedenskogo 1, Fryazino, Moscow Oblast 141190, Russia

ARTICLE INFO

Article history:
Received 18 March 2016
Received in revised form 30 September 2016
Accepted 31 October 2016
Available online 4 November 2016

Keywords:
Lead-free
Barium strontium titanate film
Ferroelectric
Polarization switching
Piezoresponse force microscopy

ABSTRACT

$Ba_{0.8}Sr_{0.2}TiO_3$ (BST 80/20) thin films with various thickness between 150 nm to 550 nm were fabricated by high-frequency reactive sputtering of a ceramic target in an oxygen atmosphere on *p*- and *n*-type Si substrates. Memory windows and effective dielectric constant of the BST film in Au/BST/Si thin film capacitors are found to be increased with the increasing thickness of the film. Surface morphology, ferroelectric domain structure, switching properties and ferroelectric activity of the BST 80/20 thin films have been investigated with the use of piezoresponse force microscopy. Complete domain switching and strong piezoresponse are found in the ferroelectric BST film. The piezoelectric coefficient (d_{33}^{eff}) and the remnant piezoelectric response (ΔPR) of BST 80/20 films are found to be increased with the thickness of the film. The conductivity type of the silicon substrate does not contribute significantly to piezoelectric and electrical properties of BST 80/20 thin films.

© 2016 Elsevier B.V. All rights reserved.

1. Introduction

Currently, ferroelectric thin films are widely used in engineering as piezoelectric transducers. At the same time, there is discussion of prospects of using ferroelectric materials in storage systems and elements of microwave technology [1–3]. Ferroelectric barium strontium titanate (BST) thin films have been widely investigated as potential materials for the applications of microelectronic devices, such as nonvolatile random access memories, infrared detectors, and microwave devices [4,5,6]. For these new applications, methods were developed and/or refined for depositing thin BST film by industry-standard and high-throughput techniques, such as RF sputtering and metal-organic chemical vapour deposition (MOCVD). The electrical properties of thin films also proved to be significantly different than bulk ceramics of the similar composition [7]. In addition, Queraltó et al. [8] demonstrated the ability of the UV laser irradiation technique combined with the chemical solution deposition for fabricating tens of nanometers thick highly crystalline epitaxial BST/LNO/LAO films in a fast way. The obtained films exhibit ferroelectric switching with perpendicular polarization comparable to similar systems produced by time-consuming conventional annealing methods. Nath et al. [9] demonstrated that multilayered ferroelectric BST films with a systematic variation in the composition (and thus the polarization) have a higher piezoelectric response compared to homogeneous samples for certain field magnitudes.

Recently, the domain contrast and local polarization switching at the nanoscale of the BST film were observed in piezoresponse force microscopy, and the results indicate the films have ferroelectric properties [10,11]. However, there is no systematic study of electrical and piezoelectric properties at nanoscale of BST 80/20 film with various thickness on silicon substrate with different type of the conductivity. It is important to understand how the film thickness affects electrical and ferroelectric properties, considering the ever-decreasing device size and the film thickness.

In this paper, we have systematically studied the thickness effect on electrical, ferro- and piezoelectric properties of BST 80/20 films with the thickness between 150 nm and 550 nm, prepared by the high frequency reactive sputtering on the Si substrate for two type conductivity (*p*- and *n*-) in order to understand its functional properties for future flash memory applications. The choice of the composition of ferroelectric $Ba_xSr_{1-x}TiO_3$ composition material is conditioned by the fact that the composition has a pronounced hysteresis of polarization by an applied voltage [1].

2. Experimental procedures

The ferroelectric $Ba_{0.8}Sr_{0.2}TiO_3$ films with a thickness of 150–550 nm were prepared by the high-frequency reactive sputtering of a ceramic target in an oxygen atmosphere on the PLAZMA-50 SE setup as described elsewhere [12]. The *p*-type and *n*-type silicon with the crystallographic orientation (100) were used as a substrate with a resistivity of about 20 Ω cm. The substrate thickness was 200 ± 2 μm. The following technological regimes were chosen for the growth of $Ba_{0.8}Sr_{0.2}TiO_3$

* Corresponding author at: National University of Science and Technology "MISiS", Leninskiy pr. 4, Moscow 119049, Russia.
E-mail address: dm.kiselev@gmail.com (D.A. Kiselev).

http://dx.doi.org/10.1016/j.tsf.2016.10.064
0040-6090/© 2016 Elsevier B.V. All rights reserved.

films: the oxygen pressure during sputtering was 60 ± 5 Pa; the distance between the target and a substrate was 10 ± 0.5 mm; the power of high-frequency discharge was 230 ± 5 W; the substrate temperature was 605 ± 5 °C; the deposition time was between 5 and 30 min. Under these conditions, the film growth rate was 15.0 nm/min. The crystallographic structure of the films obtained was investigated by X-ray diffraction as reported in the former paper [13], showing that the films possess pure perovskite structure.

For measurements of electrical properties, dot-shaped Au top electrodes with an area of ~2.7×10^{-4} cm^2 were deposited on the surface of BST films using a shadow mask by the vacuum evaporation. Capacitance-voltage (C-V) characteristics were measured at room temperature on an automated experimental setup using the LCR Agilent E4980A precision tester. Dielectric properties of BST films were evaluated from C-V characteristics of fabricated metal-ferroelectric-semiconductor capacitors (MFS capacitors).

The surface morphology and the piezoelectric response of the BST 80/20 films were measured by the scanning probe microscopy Asylum MFP-3D in the Single Frequency Piezoresponse Force Microscopy mode (PFM) [14] and Dual AC Resonance Tracking PFM (DART-PFM) [15]. We used commercial probes ASYLEC-01 with titanium-iridium conductive coating with a curvature radius of $R = 28$ nm, the resonance frequency f = 70 kHz, and the spring constant k = 2 N/m. Specifically, for the piezoelectric response (vertical piezoresponse – VPFM) measurement, thin films were grounded with a conducting layer (the *p*- and *n*-type Si substrate served as a back electrode grounded using a silver paste to the PFM stage), and then an AC bias was applied to the tip from a signal generator. The local polarization study was performed using PFM with Nanolaboratory NTEGRA Prima (NT-MDT, Russia). A DC voltage of amplitude 40 V was applied between the tip and the ground electrode, while the sample surface was scanned. After each poling scan, the same area was imaged in the PFM mode to see whether the PFM contrast was changed locally.

3. Results and discussion

The microstructure, such as average lateral grain size and a surface roughness, is one of the key parameters determining the electrical properties of the high dielectric thin film capacitor. Fig. 1 (a) shows the cross-sectional view of the SEM image of the BST thin film. The thickness of the BST film was about 350 nm. Fig. 1 (b) shows the atomic force microscopy image of the BST 80/20 thin film deposited at the optimum deposition conditions. The microstructure showed uniformly distributed grains. The average lateral grain size of the BST 80/20 film with thickness 350 nm was 47 nm; the root mean square (Rms) surface roughness measured over an area of 1.5×1.5 μm^2 was 2.8 nm. This procedure was made for all investigated thin films. Table 1 summarizes the statistical parameters for as-grown BST 80/20 films in the present work. As shown in Table 1, without exception, parameters of Rms and the lateral grain size increase with BST film thickness for both types of Si substrate. This result suggests that there is a correlation between the morphology and the dielectric properties of these films, as will be shown below.

Table 1
Root mean square (Rms) surface roughness, lateral grain size obtained from atomic force microscopy images of BST 80/20 thin films for different thickness.

Thickness (nm)	*p*-type Si substrate		*n*-type Si substrate	
	Rms (nm)	Lateral grain size (nm)	Rms (nm)	Lateral grain size (nm)
150	1.5	31	2.2	28
250	2.3	35	2.8	33
350	2.8	45	3.2	41
450	3.6	52	3.5	48
550	4.9	65	4.2	58

Fig. 2 (a) shows typically C-V curves of the MFS structures (Au/BST(350 nm)/Si) fabricated on *p*-type, and *n*-type Si substrates at a frequency of 100 kHz. The bias voltage was varied from –20 V to 20 V and back with the step 0.1 V. The curves clearly show the regions of the accumulation, depletion, and inversion. The clockwise (or counterclockwise) direction of the curve reveals that the MFS capacitor structure had a good ferroelectric polarization switching property. In our case, the C-V characteristics of the BST 80/20 sputtered on *p*-type Si substrate show a hysteresis loop with a counterclockwise rotation, and in the case of the *n*-type Si substrate – in the clockwise direction. This mode of switching is the desired mode for the memory operation. In addition, the flat-band voltage for both samples was slightly shifted towards the positive voltage, which may be due to built-in immobile charges associated with ionic defects in the ferroelectric thin film. In addition, a hysteresis in the C-V curve indicates a memory window related to a coercive field of the ferroelectric material [16]. Fig. 2(b) summarizes the memory windows of the MFS structures as a function thickness of BST layer for both types of Si substrates. The memory windows are determined with the difference of flat-band voltages in the forward and reverse C-V curves. As it can be seen from the data, the memory windows increase with the increase of the BST film thickness and ultimately tend to saturation. The effective dielectric constant of BST films used in the multilayered capacitor Au/BST/Si has a linear dependence from the BST film thickness (Fig. 2c). The effective dielectric constant for BST thin films deposited on *n*-type Si substrate is slightly smaller than for *p*-type Si. It should be noted that the change of the effective permittivity (Fig. 2c) of the film thickness and the shape of hysteresis loops of BST structures on *p*- and *n-Si*-substrates are almost identical. These circumstances may indicate that the conductivity type of silicon substrate does not affect the quality and the structure of BST films.

The results obtained show that dielectric properties measured in the kHz range are strongly influenced by the grain size. Increase of the grain size with increasing BST layer thickness coincides with the increase of permittivity, in agreement with the dielectric grain size effect. Pečnik et al. [17] have shown that for the BST 50/50 thin film when the film thickness increased from 90 to 170 nm, the average lateral grain size increased from 45 to 87 nm, and the dielectric permittivity of films

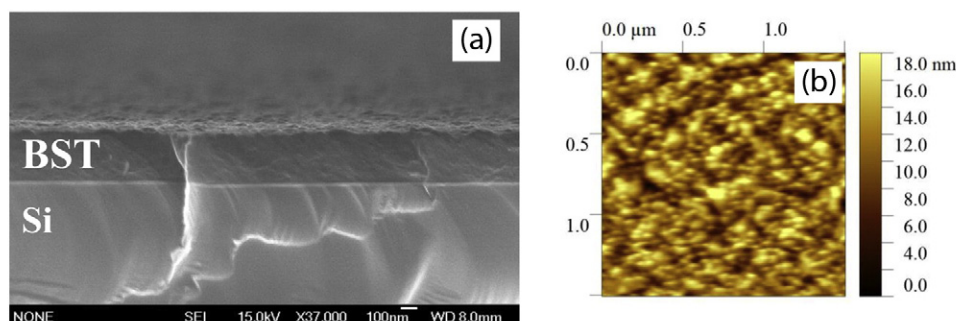

Fig. 1. The Cross-sectional view of the SEM image (a) and the 2D AFM topography image (b) of the BST 80/20 thin film deposited on the p-type Si substrate.

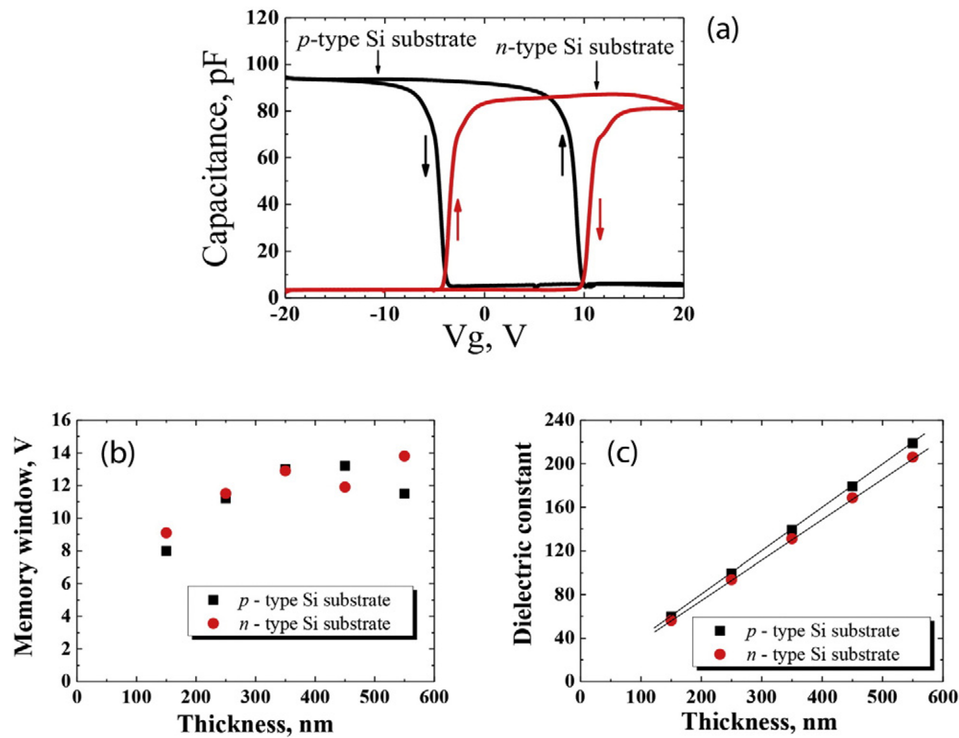

Fig. 2. C-V characteristics of the BST(350 nm)/p-type Si and the BST(350 nm)/n-type Si MFS structure (a), summary memory windows of the MFS (b) and the effective dielectric constant (c) of BST 80/20 thin films as a function of the film thickness.

increased from 650 to 1250, measured at 100 kHz and the room temperature. The tensile residual stress, which develops as a consequence of the thermal expansion mismatch between the substrate and the film, is high and increases with increasing thickness [17].

Fig. 3 shows the temperature dependence of the dielectric constant of the BST 80/20 (350 nm thick) films for both types of Si substrates. It was observed that the dielectric constant of the BST thin film (115 (*n*-type Si) and 122 (*p*-type Si)) is much lower than nanostructured ceramic BST 80/20 (e.g., 800 at room temperature) [18]. Around 60 °C (Curie temperature), a transition from the ferroelectric phase to the paraelectric phase is noted for BST 80/20 film deposited on *p*-type Si substrate. The broad peak in the response of ferroelectric films can be attributed to the mechanical and electrical strains in the films. It was also observed that the dielectric constant monotonically decreases with the temperature for BST 80/20 sputtered on *n*-type Si substrate. The dramatic variation in Curie temperature can be related to the small grain size (see Table 1). It is

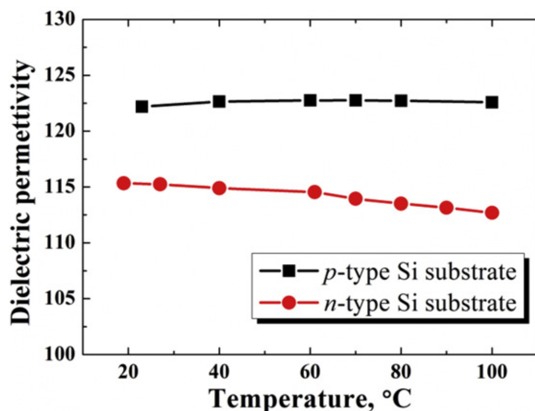

Fig. 3. The temperature dependence of the dielectric constant at 100 kHz for BST(350 nm)/*p*-type Si and BST(350 nm)/*n*-type Si substrates.

well known that the properties of polycrystalline ferroelectrics are dependent on microstructure, particularly with respect to grain size. Lines and Glass studied the bulk BST ceramic dependence of T_C or ε and suggested that T_C was greatly dependent on the crystallite size [19].

PFM images of the ferroelectric behavior of BST 80/20 350-thick film were obtained through DART-PFM as a response to the bias voltage (2 V_{AC}) at the room temperature as shown in Fig. 4(a–c). These figures consisted of the topography, as well as the PFM amplitude and the PFM phase images, which reveal information on the local electromechanical response and the out-of-plane ferroelectric domain distribution. Fig. 4(d) represents the results of the polarization reversal through local hysteresis loops on the BST 80/20 film deposited on the *p*-type Si substrate. The domain switching in two directions was successfully achieved. Asymmetries in amplitude and phase loops also point to the existence of defects, since the asymmetries are known to be associated with an internal field created by non-uniformly distributed charged defects [20].

Fig. 5(a, b) shows piezoelectric hysteresis loops as a function of different thicknesses of the BST 80/20 film for both types of the conductivity of Si substrates. The films present well-known butterfly curves for the variation of the VPFM amplitude versus the voltage. All amplitude curves also confirm the existence of switchable intrinsic polarization in the BST 80/20 film.

As it can be seen from the loops, the value of maximum amplitude and the slope increased with increasing BST layer thickness. The piezoelectric coefficient $d_{33}^{eff}$was calculated from the slope of the linear region of the loop of the non-biased butterfly curves [21]. Table 2 summarizes the value of piezoelectric coefficient d_{33}^{eff} for all BST samples obtained from VPFM amplitude loops. The effective piezoelectric coefficient d_{33} of the 150 nm thick BST film is about 4–5 pm/V, which has good agreement with the value obtained on the 130.5 thick BST film (3 pm/V) [22]. For BST 80/20 films sputtered on *p*-type and *n*-type Si substrates, we observed an increasing value of effective piezoelectric constant d_{33}^{eff} with the film thickness. This increase is associated with the surface strain and the effect of interface between the ferroelectric and the substrate.

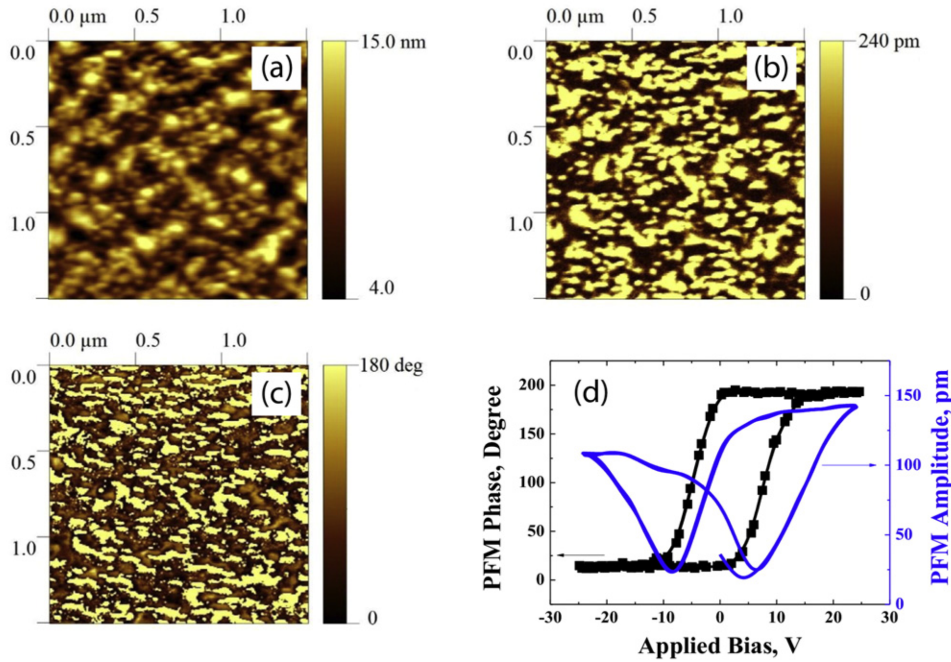

Fig. 4. The typically topography (a) and piezoresponse force microscopy amplitude (b) and (c) phase images for BST 80/20 film 350 nm-thick on the p-type Si substrate. PFM hysteresis loops (d) – Phase and Amplitude signals.

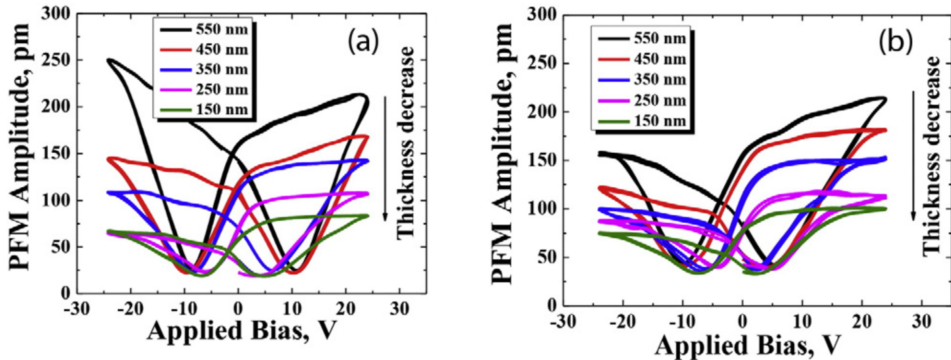

Fig. 5. Local PFM amplitude hysteresis loops for BST 80/20 thin films: *p*-type (a) and *n*-type (b) Si substrates.

Ferroelectricity in all BST 80/20 thin films was investigated by vertical PFM. As example, Fig. 6(a) presents the switching experiment on the as-grown BST 80/20 thin film (on *p*-type Si substrate) with a thickness of 350 nm. For all BST films, local poling was successful by applying ± 40 V DC while scanning an area of 10×10 μm^2, which created a strong bright (left side at $+40$ V) and dark (right side at –40 V) contrast in VPFM image. We removed offset for all VPFM images for better image clarity. However, our recent experimental results on piezoelectric response of BST 80/20 films [4] indicate that the BST film has self-polarization effect. This effect is not discussed in the current paper.

Table 2
The piezoelectric coefficient d_{33}^{eff} of BST 80/20 thin films sputtered onto *p*- and *n*-type Si (100) substrate.

Thickness, nm	d_{33}^{eff}, pm/V (*p*-type Si substrate)	d_{33}^{eff}, pm/V (*n*-type Si substrate)
150	4	5
250	6	6.5
350	8	7
450	12	9
550	15	10

Fig. 6(b) shows the cross-sectional data of the piezoresponse signal changes across the center PFM image included in as-grown state and poling area. Based on this graph, we calculate the average remnant piezoresponse signal (ΔPR) as the difference between the amplitude for positive and negative poling areas. For the BST 80/20 film with a thickness of 350 nm, ΔPR value was 780 pA. Thus, we have defined ΔPR values for all investigated BST thin films with different thickness and both types of Si substrates. Fig. 7 summarizes this data.

Increasing value of the remnant piezoresponse with a thickness of the BST film confirms the result observed in relation to d_{33}^{eff} for these films (Fig. 5 and Table 2). Similar phenomena are observed in the ultrathin $BiFeO_3$ films grown on STO (001) substrate with a $La_{0.67}Sr_{0.33}MnO_3$ cover layer [23] and in epitaxial PZT ultrathin films 50–500 Å thick grown on SRO buffered (100) STO substrate by pulsed laser deposition [24], where it was shown that this apparent contradiction between the structural measurements and the measured switchable polarization was explained by an increasing presence of a strong depolarization field, which created a pinned 180° polydomain state for the thinnest films. In addition, the remnant piezoresponse for BST thin films deposited on the *n*-type Si substrate is slightly smaller than for the *p*-type Si substrate.

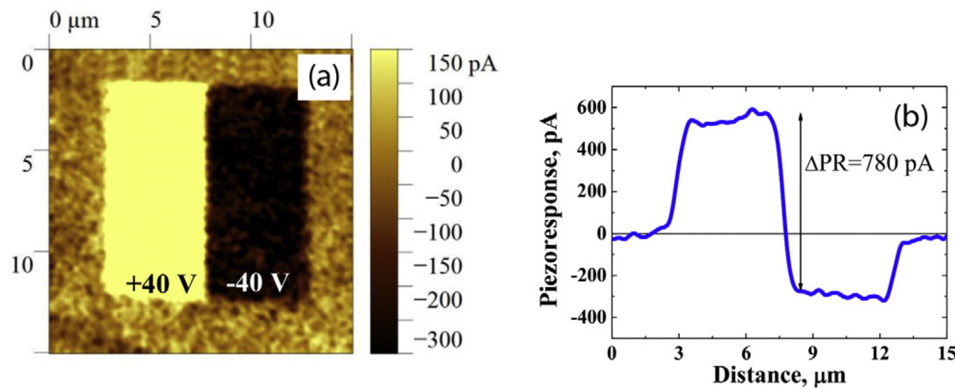

Fig. 6. The piezoresponse image (a) obtained by applying a DC bias voltage (positive and negative) to the BST 80/20 film and the cross-section profile (b) of the piezoresponse signal along a center scan in (a).

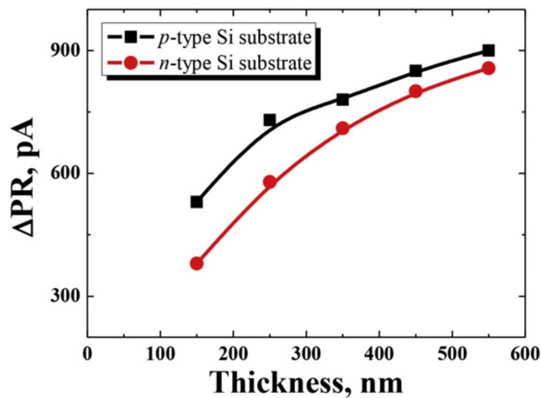

Fig. 7. Remnant PFM signal as a function of the film thickness for the BST 80/20 sputtered on *p*- and *n*-type Si substrates.

4. Conclusions

Summarizing our research, polycrystalline $Ba_{0.8}Sr_{0.2}TiO_3$ thin films with a thickness ranging from 150 nm to 550 nm were prepared on Si substrates (the *p*- and *n*-type conductivity) by the RF magnetron sputtering. AFM illustrated that the deposition time or thickness had an influence on the surface morphology and lateral grain sizes of BST 80/20 films. The MFS structure (Au/BST/Si) showed hysteretic characteristics in the C-V plot with a typical window memory, and this parameter depended from the film thickness. Increasing the thickness would result in an increase in the dielectric constant, which mainly stems from dielectric grain size effect and the interfacial-layers effect. The piezoelectric coefficient (d_{33}^{eff}) and the remnant piezoelectric response (ΔPR) of BST 80/20 films are found to be increased with the increasing thickness of the film. Our studies on ferroelectric BST 80/20 thin films therefore indicate that although ferroelectricity is maintained down to hundred nanometer level thickness, switchable polarization (value of ΔPR) is severely affected, while the type of the conductivity of the silicon substrate does not contribute significantly to the piezoelectric and electrical properties of BST films.

Acknowledgments

The studies are performed on the equipment of Center for Shared Use “Materials Science and Metallurgy” at the National University of Science and Technology “MISiS”. The study was supported in part by the Russian Foundation for Basic Researches (projects 16-07-00665 and 16-07-00666).

References

[1] Y.V. Gulyaev, A.S. Bugaev, A.Y. Mityagin, G.V. Chucheva, M.S. Afanasev, Aspects of using of ferroelectric materials for microwave devices, Achievements of Modern Radioelectronics, 12, 2011, pp. 3–9.
[2] K.A. Vorotilov, A.S. Sigov, A.A. Romanov, P.R. Mashevich, Formation of ferroelectric heterostructures with controlled nanostructures for micro- and nanoelectronic devices, Nanotechnology: development and applications - XXI century 4 (2012) 4–13.
[3] K.A. Vorotilov, A.S. Sigov, Ferroelectric memory, Phys. Solid State 54 (2015) 894–899.
[4] D.A. Kiselev, M.S. Afanasiev, S.A. Levashov, G.V. Chucheva, Growth kinetics of induced domains in $Ba_{0.8}Sr_{0.2}TiO_3$ ferroelectric thin films, Phys. Solid State 57 (2015) 1151–1156.
[5] R. Balachandran, B.H. Ong, H.Y. Wong, K.B. Tan, M.M. Rasat, Dielectric characteristics of barium strontium titanate based metal insulator metal capacitor for dynamic random access memory cell, Int. J. Electrochem. Sci. 7 (2012) 11895–11903.
[6] K. Nadaud, C. Borderon, R. Gillard, E. Fourn, R. Renoud, H.W. Gundel, Temperature stable $BaSrTiO_3$ thin films suitable for microwave applications, Thin Solid Films 591 (2015) 90–96.
[7] C. Basceri, S.K. Streiffer, A.I. Kingon, R. Waser, The dielectric response as a function of temperature and film thickness of fiber textured $(Ba,Sr)TiO_3$ thin films grown by chemical vapor deposition, J. Appl. Phys. 82 (5) (1997) 2497–2504.
[8] A. Queraltó, A. Pérez del Pino, M. de la Mata, J. Arbiol, M. Tristany, A. Gómez, X. Obradors, T. Puig, Growth of ferroelectric $Ba_{0.8}Sr_{0.2}TiO_3$ epitaxial films by ultraviolet pulsed laser irradiation of chemical solution derived precursor layers, Appl. Phys. Lett. 106 (2015) 262903.
[9] R. Nath, S. Zhong, S.P. Alpay, B.D. Huey, M.W. Cole, Enhanced piezoelectric response from barium strontium titanate multilayer films, Appl. Phys. Lett. 92 (2008) 012916.
[10] A.N. Kuskova, R.V. Gainutdinov, O.M. Zhigalina, Influence of thickness on the domain structure of barium-strontium-titanate films on MgO substrates, J. Surf. Invest.: X-Ray, Synchrotron Neutron Tech. 8 (4) (2014) 761–766.
[11] L. Guiying, Y. Ping, X. Dingquan, Ferroelectric properties of $Ba_{1-x}Sr_xTiO_3$ thin films synthesized by using novel sol–gel technique through carbonates, J. Electroceram. 21 (2008) 340–343.
[12] M.S. Ivanov, M.S. Afanas'ev, Specific features of the formation of $Ba_xSr_{1-x}TiO_3$ ferroelectric thin films on different substrates by radio-frequency sputtering, Phys. Solid State 51 (7) (2009) 1328–1331.
[13] M.S. Afanasev, A.V. Byrov, V.K. Egorov, P.A. Lychnikov, G.V. Chucheva, Technological control of element structure perovskite layer of planar nano structures deposited in HF-plasma, Science Intensive Technologies 13 (5) (2012) 53–57.
[14] A.L. Gruverman, J. Hatano, H. Tokumoto, Scanning force microscopy studies of domain structure in $BaTiO_3$ single crystals, Jpn. J. Appl. Phys. Part 1 36 (4A) (1997) 2207–2211.
[15] B.J. Rodriguez, C. Callahan, S.V. Kalinin, R. Proksch, Dual-frequency resonance-tracking atomic force microscopy, Nanotechnology 18 (47) (2007) 475504.
[16] H.N. Lee, Y.T. Kim, Y.K. Park, Memory window of highly c-axis oriented ferroelectric $YMnO_3$ thin films, Appl. Phys. Lett. 74 (1999) 3887–3889.
[17] T. Pečnik, S. Glinšek, B. Kmet, B. Malič, Combined effects of thickness, grain size and residual stress on the dielectric properties of $Ba_{0.5}Sr_{0.5}TiO_3$ thin films, J. Alloys Compd. 646 (2015) 766–772.
[18] V.R. Mudinepalli, L. Feng, W.-C. Lin, B.S. Murty, Effect of grain size on dielectric and ferroelectric properties of nanostructured $Ba_{0.8}Sr_{0.2}TiO_3$ ceramics, Journal of Advanced Ceramics 4 (1) (2015) 46–53.
[19] M.E. Lines, A.M. Glass, Principles and Applications in Ferroelectrics and Related Materials, Clarendon, Oxford, UK, 1977 531.
[20] D. Zhou, J. Xu, Q. Lu, Y. Guan, F. Cao, X. Dong, J. Müller, T. Schenk, U. Schröder, Wake-up effects in *Si*-doped hafnium oxide ferroelectric thin films, Appl. Phys. Lett. 103 (2013) 192904.

[21] C.M. Bedoya-Hincapié, E. Restrepo-Parra, J.J. Olaya-Flórez, J.E. Alfonso, F.J. Flores-Ruiz, F.J. Espinoza-Beltrán, Ferroelectric behavior of bismuth titanate thin films grown via magnetron sputtering, Ceram. Int. 40 (2014) 11831–11836.
[22] S.R. Kwon, W. Huang, L. Shu, F.-G. Yuan, J.-P. Maria, X. Jiang, Flexoelectricity in barium strontium titanate thin film, Appl. Phys. Lett. 105 (2014) 142904.
[23] J.L. Zhao, H.X. Lu, J.R. Sun, B.G. Shen, Thickness dependence of piezoelectric property of ultrathin $BiFeO_3$ films, Physica B 407 (2012) 2258.
[24] V. Nagarajan, J. Junquera, J.Q. He, C.L. Jia, R. Waser, K. Lee, Y.K. Kim, S. Baik, T. Zhao, R. Ramesh, P. Ghosez, K.M. Rabe, Scaling of structure and electrical properties in ultrathin epitaxial ferroelectric heterostructures, J. Appl. Phys. 100 (2006) 051609.